Taximaimaiti *et al.*
BMC Complementary Medicine and Therapies (2023) 23:222
https://doi.org/10.1186/s12906-023-04025-5

BMC Complementary Medicine and Therapies

RESEARCH

Open Access

Rapid identification of chemical components in Xuelian granule by UHPLC-Q-orbitrap-HRMS based on enzyme activity in vitro

Xiatiguli Taximaimaiti[1,2], Rahima Abdulla[1], Xuelei Xin[1], Yuan Zhao[3], Yi Liu[3], Haji Akber Aisa[1], Deqiang Deng[3*] and Tao Wu[1*]

Abstract

Background Xuelian granule (XL), a traditional Chinese medicine (TCM) formula, has been used for the treatment of diabetic nephropathy for a long time as a hospital preparation. Because the active ingredients in the XL that can help to treat diabetic nephropathy are still unclear, which limits the interpretation for its pharmacological mechanism, further development and subsequent study on the material basis of its efficacy.

Methods In this study, a screening method based on inhibition activity against aldose reductase (AR) was employed for activity-directed chemical analysis of XL using ultra-high performance liquid chromatography combined with quadrupole-orbitrap high resolution mass spectrometry (UHPLC-Q-orbitrap-HRMS) technique.

Results A total of 178 compounds, including 46 terpenes, 47 organic acids, 25 flavonoids, 29 phenylethanoid glycosides, and 31 other types, were tentatively identified from XL which might responsible for its AR inhibition activity.

Conclusion This is the first study for a systematic, rapid, and accurate qualitative analysis of XL. This research provides a scientific and experimental basis for further researches on pharmacodynamics material basis and quality control of XL.

Keywords Aldose reductase, Chemical profile, Xuelian granule, Liquid chromatography-mass spectrometry

Background

Diabetic nephropathy (DN) is one of the most common chronic complications of diabetes mellitus, with an incidence of over 40% [1]. The high mortality associated with DN has become an increasingly serious problem [2, 3]. Nowadays, traditional Chinese medicine (TCM) has become a focus in the treatment of DN due to its better efficiency, high safety and low cost [4, 5]. Xuelian granule (XL), a classical TCM prescription, has been used by Urumqi TCM Hospital as a hospital preparation for the treatment of DN for many years. It consists of twelve crude herbs, with Saussureae Involucratae Herba (SH), Cibotii Rhizima (CRH), Cyathulae Radix (CR), Eucommiae Cortex (EC), Astragali Radix (AsR), Paeoniae Radix Alba (PRA), Salviae Miltiorrhizae Radix et Rhizoma (SRR), Poria, Moutan Cortex (MC), Cistanches Herba (CDH), Paeoniae Radix Rubra (PRR), Centellae Herba (CH). According to the clinical data provided by the hospital, XL treatment shows very significant effect.

*Correspondence:
Deqiang Deng
523560771@qq.com
Tao Wu
wutao@ms.xjb.ac.cn
[1] The State Key Laboratory Basis of Xinjiang Indigenous Medicinal Plants Resource Utilization, and Key Laboratory of Chemistry of Plant Resources in Arid Regions, Xinjiang Technical Institute of Physics and Chemistry, Chinese Academy of Sciences, Urumqi 830011, China
[2] University of Chinese Academy of Sciences, Beijing 100049, China
[3] Urumqi Hospital of Traditional Chinese Medicine, Urumqi 830000, China

The main therapeutic effect of XL is to improve kidney function by reducing the creatinine and urea nitrogen of patients.

Generally, the most significant features of TCM are multi-components and multi-effects that including a great number of compounds with various chemical structures and biological activities [6–8]. As a TCM prescription, rapid screening and recognition of active ingredients in XL is rather challenging, due to the diversity and complexity of its chemical components. Therefore, to date, there are no reports on overall chemical composition of XL. The uncertainty in chemical constituents of XL resulted in the lack of relevant studies, which restricted to clarify its mechanism of action, comprehensive development, and extensive application in the clinic. Thus, it is necessary to establish a systematic and comprehensive analytical method for the investigation of chemical components in XL to identify the active ingredients and its pharmacodynamic material basis.

AR is widely recognized important factor in the process of the occurrence and development of DN [9–11]. To date, a wide range of synthetic and natural AR inhibitors have been developed. Such as bis-sulfide and its derivatives [12], acylthiourea derivatives [13], N-substituted phthalazine sulfonamide derivatives [14], these synthetic compounds and its derivatives showed AR enzyme inhibitory activity in vitro at different degrees. Furthermore, natural phenolic compounds, including acteoside, echinacoside, danshensu and vanillic acid, displayed inhibition effects against AR as well [15, 16]. According to the previous studies on individual herbs in XL, the chemical components, such as acylated phenylethanoid glycosides from CHD [17], paeoniflorins from MC [18], Astragalus saponin from AsR [19], tanshinone I and IIA from SRR [20], flavonoids like kaemferol and quercetin [21], have displayed AR inhibition activities to some extent. For the efficiency and rapidity of chemical analysis, the screening mode on AR inhibition activity was employed for different enrichment parts of XL. Besides, ultra-high performance liquid chromatography coupled with quadrupole-orbitrap high resolution mass spectrometry (UHPLC-Q-Orbitrap-HRMS) is a suitable technique for the complex and diverse chemical component analysis of TCMs, because of its characteristics of high resolution, excellent sensitivity, accurate precursor and fragment ions information [22–24].

In this study, XL water extract was subjected to alcohol precipitation and resulted to supernatant and precipitate samples. After the in vitro AR inhibition activity screening of the three samples (XL water extract, supernatant, precipitate sample), we found that supernatant sample showed stronger AR inhibition activity compared to precipitate sample and whole water extract of XL. Subsequently, in order to explore active components in the prescription, the chemical ingredients in the supernatant sample were systematically characterized using UHPLC-Q-orbitrap-HRMS method. It is hoped to provide a methodological reference for the exploration of complex prescriptions in an activity-directed manner, as well as a solid chemical substance basis for the further research on the quality control, pharmacodynamics and wide-ranging clinical practice of XL.

Methods

Chemicals and materials

HPLC–MS grade methanol and acetonitrile were supplied by Fisher Scientific (Fair Lawn, NJ, USA). Chromatographic grade formic acid was obtained from Merck (Darmstadt, Germany). Deionized water was purchased from Watson's (Hong Kong, Ltd., China). All the 12 herbs of XL were purchased from Xinjiang Jiu-Yuan-Tang traditional Chinese medicine Co., Ltd. (Urumqi, Xinjiang, China).

The reference standards of gallic acid (110,831–201,605), protocatechuic acid (110,809–201,906), 5-*O*-caffeoylquinic acid (110,753–201,515), pinoresinol diglucoside (p0216), echinacoside (111,670–201,907), quercitrin (111,538–201,606), rutin (100,080–201,610), isoquercitrin (111,809–201,403), quercetin (111,081–201,408), cyasterone (11,804–201,705), tanshinone I (110,867–201,607), cryptotanshinone (110,852–201,807), paeoniflorin (110,736–201,943), asiaticoside (110,892–201,504), madecassoside (110,893–201,804) (≥98% purity) were provided from the Chinese Food and Drug Accreditation Institute (Shanghai, China); calycosin-7-*O*-glucoside (p0616), acteoside (21,090,906), kaempferol (p0013), paeonol (p0058), salvianolic acid B (p0132), tanshinone IIA (p0019), astragaloside IV (p0140), 1,5-*O*- dicaffeoylquinic acid (16,040,105) (≥98% purity) were obtained from Shanghai Chunyou Biotechnology (Shanghai, China); 3-*O*-caffeoylquinic acid (GSB 11–3796-2020), 4-*O*- caffeoylquinic acid (GSB 11–3795-2020), 1,3-*O*- dicaffeoylquinic acid (GSB 11–3791-2020), 3,4-*O*- dicaffeoylquinic acid (GSB 11–3792-2020), 3,5-*O*- dicaffeoylquinic acid (GSB 11–3793-2020), 4,5-*O*-dicaffeoylquinic acid (GSB 11–3794-2020), (≥98% purity) were provided by Key Laboratory of Plant Resources and Chemistry in Arid Regions (Urumqi, Xinjiang, China).

AR was expressed by laboratory from the Xinjiang Technical Institute of Physics and Chemistry (Urumqi, Xinjiang, China).

Sample preparation

XL water extract

XL water extract was prepared according to its original record in the prescriptions of Urumqi TCM Hospital.

Each crude herbs were approximately weighed as follows: SH 20 g, CRH 12 g, CR 12 g, EC 12 g, AsR 20 g, SRR 12 g, Poria 12 g, MC 9 g, PRA 12 g, PRR 12 g, CDH 12 g, CH 20 g. Herbal materials were mixed and extracted by heating reflux method for 3 times with mass-liquid rario of 1:12 for 2 h. After cooling down, the whole extract was filtered and merged, and then enriched to 150 mL (approximate equal for 1 g crude herb/mL). Finally, extract powder was prepared via vacuum drying at 60 ℃. The supernatant and precipitate parts: the alcohol precipitation method was used for the enrichment of the small molecular components in supernatant, and large molecular components in precipitate, respectively. The above XL water extract was completely dissolved in water, and then added a ratio of 1:4 95% ethanol, mixed, and stored at 4℃ for a night. The solution was filtrated in the next day, and the supernatant solution was concentrated and dried for using as supernatant part. Precipitate was dried by vacuum drying at 60 ℃ directly for using as precipitate part. Different samples of XL were dissolved in distilled water, and filtered with a 0.22 μm membrane before detection.

AR inhibitory assay

The inhibition activity of XL three different samples against AR was determined under the optimal reaction conditions described in methods of Ye Ma et al. [25]. Briefly, 4 μL DMSO or samples, 146 μL potassium phosphate (PBS) and 10 μL hAR solution were successively added to 96-well plates for a total volume of 160 μL. Subsequently, 40 μL mixtures of 2 mM NADPH and 10 mM DL-glyceraldehyde (1:1, V/V) were added immediately to standard well and 40 μL potassium phosphate (PBS) for standard blank well. After 40 min of incubation at 25 ℃, absorbance was obtained at 340 nm (A_{340}) with an ELISA instrument. The AR inhibition ratio (%) was figured up based on the following equation (Eq. 1):

$$\text{AR inhibition (\%)} = \left[1 - \frac{[(N_1 - N_0) - (S_1 - S_0)]}{[(N_1 - N_0) - (E_1 - E_0)]}\right] \times 100\% \quad (1)$$

where N_1, N_0, S_1, S_0, E_1 and E_0 represent the absorbance of the negative test group (combination of PBS and substrate), the negative control group (just PBS only), the sample test group (combination of sample, PBS, and enzyme), the sample control group (combination of just sample and PBS), the enzyme test group (combination of PBS, substrate and enzyme) and the enzyme control group (combination of just PBS and enzyme), respectively.

Taking the mean ± standard deviation to express all experimental data, and at least three parallel tests were conducted for each condition. GraphPad Prism (version 8.0.1; GraphPad Software, La Jolla, CA, USA) was used for the in vitro data analysis with a significance of $P < 0.05$.

Rapid characterization of active components in XL

An Ultimate 3000 system (Thermo Fisher Scientific Co., Germany) coupling with a quadrupole/orbitrap high resolution mass spectrometry (Q-Exactive, Thermo Fisher Scientific Co., Germany) was used for ultra-high performance liquid chromatography analysis. A Waters XBridge C_{18} column (250 × 4.6 mm, 5 μm, Waters, USA) was applied for chromatographic analysis in a 1.0 mL/min of flow rate, using the combination of 0.1% formic acid (V/V) in water (A) and acetonitrile (B) as a mixed mobile phase. A gradient elution process was used as below: 0–10 min, 3% B; 10–13 min, 3% ~ 4% B; 13–23 min, 4% ~ 12% B; 23–35 min, 12% ~ 18% B; 35–50 min, 18% ~ 25% B; 50–60 min, 25% ~ 30% B; 60–65 min, 30%-90% B; 65–75 min, 90% B. The chromatographic analysis was conducted at 30 ℃ of column temperature with 10 μL of sample injection volume. The UV absorption was monitored at the full-scan mode (190–850 nm). MS detection was adopted scan range with 100–1500 mass-to-charge ratio (*m/z*) in both the positive and negative ionization modes. The parameters of the electrospray ionization (ESI) source were as follows: heating temperature 300 ℃; capillary temperature 350 ℃; auxiliary gas flow 10 arb; sheath gas flow 40 arb, voltage 3.5 kV in positive mode; sheath gas flow 38 arb, voltage 2.8 kV in negative mode; The stepped normalized collision energy (NCE) was set between 30, 50, or 70; Full mass resolution ratio at 70,000 (FWHM); dd-MS^2 of 17,500 (FWHM).

Results

AR activity assay

The AR inhibition activity test was measured on different parts of XL. The results showed that the supernatant of XL exhibited strong AR inhibitory action in a dose-dependent manner with IC_{50} value of 75.13 ± 10.16 μg/mL, while the water extract and precipitates of XL showed lower inhibition activity against AR (shown in Fig. 1a and b). Therefore, the supernatant of XL was used for chemical analysis.

Characterization and identification

For the chemical ingredients analysis of XL supernatant part, UHPLC-Q-orbitarp-HRMS method was employed to obtain retention time (Rt), precise mass spectra, and MS/MS information. The total ion chromatography (TIC) was observed in both positive and negative ion modes (shown in Fig. 2), and the concrete

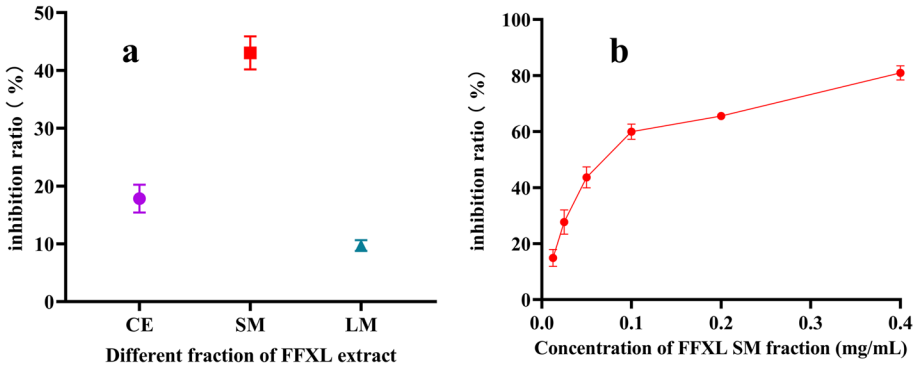

Fig. 1 AR inhibition activity of XL granule in vitro. The inhibition activity of different parts of XL at concentration of 100 μg/mL **a**; The inhibition activity of XL supernatant part at different concentrations with IC50 values of 75.13 ± 10.16 μg/mL **b**

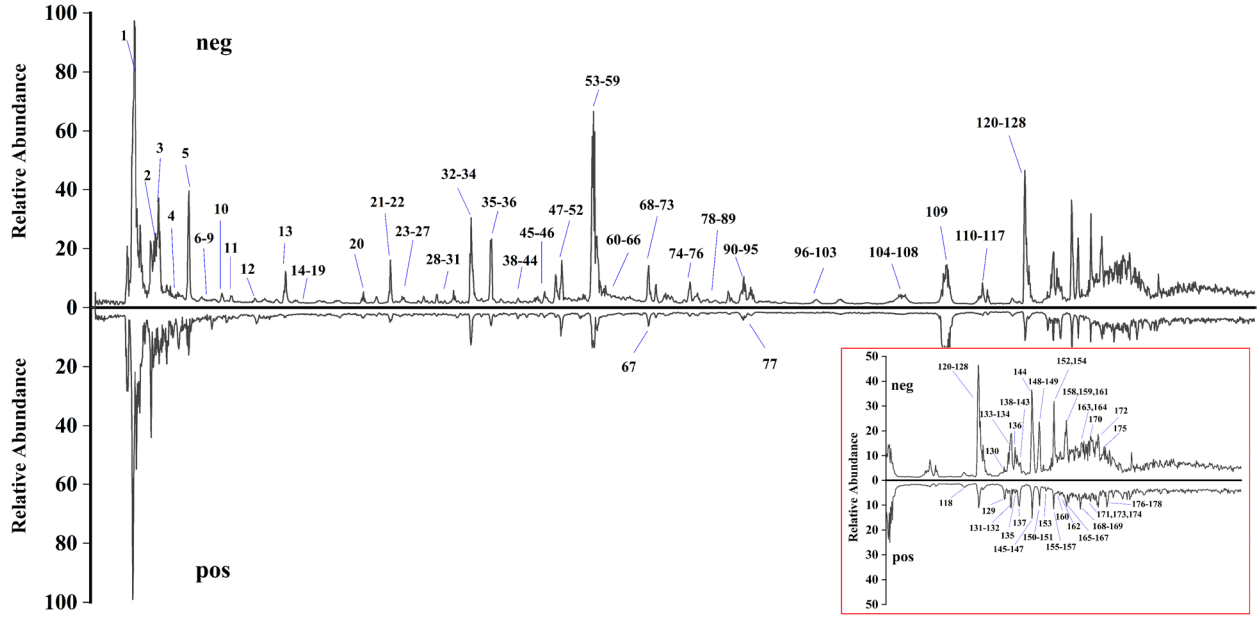

Fig. 2 The total ion chromatograms (TIC) of XL supernatant part by UHPLC-Q-orbitrap-HRMS. neg: TIC in negative mode, pos: TIC in positive mode

MS data of compounds were summarized in Table S1. To characterize the compound structures, the precision mass, MS/MS information and fragmentation pathways were compared to the relevant references, online databases, and reference standards with mass errors < 5 ppm. Xcalibur version 4.2 software (Thermo Fisher Scientific, Waltham, MA, USA) was applied for the evaluation of all MS data analysis. A total of 178 compounds, including 46 terpenoids, 47 organic acids, 25 flavonoids, 29 phenylethanoid glycosides, and 31 other types, were analyzed and characterized. Among which 29 compounds were clearly confirmed by comparing the fragmentation data and retention time with reference standards.

Characterization of terpenoids

A total of 46 terpenoids considered to widely exist in natural plants were tentatively identified from XL, including 24 monoterpene, 10 diterpenes, 7 triterpenes and 5 iridoids.

Monoterpenes were special compounds in XL, which were presumably derived from MC, PRA, PRR [26–28]. There are two types of monoterpenes in XL, including paeoniflorin and albiflorin. A total of 24 monoterpenes

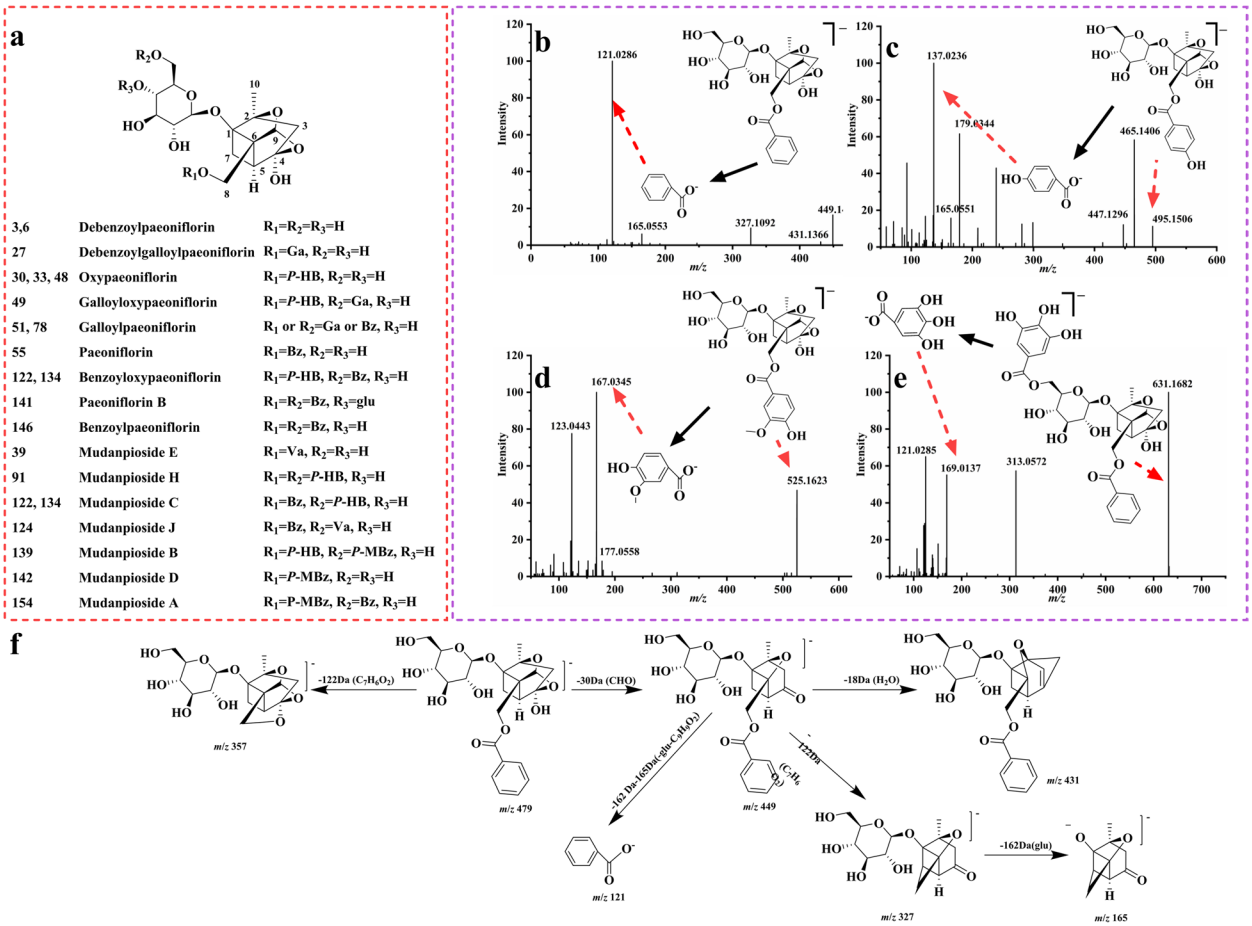

Fig. 3 The chemical structures of monoterpenes **a**, the MS/MS spectra of paeoniflorin **b**, oxypaeoniflorin **c**, mudanpioside **d**, galloylpaeoniflorin **e**, and detailed fragmentation pathways of paeoniflorin **f** in negative ion mode

were found in XL, the main chemical structures and fragmentation pattern was illustrated in Fig. 3. The similarity in molecular structure of paeoniflorins (Fig. 3a) resulted in the same fragmentations in mass spectrometry. The product ion of *m/z* 165 resulted from the basic pinane structure, was a special product ion in monoterpenes MS/MS spectra. A series number of characteristic fragments generated at *m/z* 121, 137, 169, 167 and 151, which are from different functional groups, including benzoic acid (Bz), *p*-hydroxybenzonic acid (*P*-HBz), gallic acid (Ga), vanillic acid (Va), and *p*-methoxybenzoic acid (*P*-MBz) respectively (shown in Fig. 3b, c, d, e). In addition, there were some common fragment ions produced from the loss of neutral fragments of CHO (30 Da), H_2O (18 Da), CO_2 (44 Da), glucose (162 Da). For compound **55** as an example, the main cleavage mechanism of monoterpenes in XL was illustrated (Fig. 3b and f). Its precursor ion of *m/z* 525.1622 in $[M\text{-}H+COOH]^-$ was more clear than of *m/z* 479.1566 ($C_{23}H_{28}O_{11}$, error 3.6881 ppm) in $[M\text{-}H]^-$ with the retention time of 32.32 min. In MS/MS spectra, the fragments at *m/z* 449.1471 and 327.1092 was clearly observed, that was caused by successive loses of a CH_2O (30 Da) and a benzoic acid part (122 Da) which is connected with pinane skeleton at C-8 position. Furthermore, the fragments at *m/z* 165.0553 and 121.0286 were more particular ions that could be found in almost all paeoniflorins' MS/MS spectra, which were assignable to fragments of pinane skeleton and benzoic acid part respectively. According to the above mentioned characteristic fragmentations, and combining with the fragmentation pathways of reference standard, compound **55** was clearly marked as paeoniflorin.

Diterpenes (compound **157**, **168**, **169**,**172**, **173**, **174**, **175**, **176**, **177**, **178**) in XL belonged to tanshinones class which were mainly from SRR, including Tanshinone I, IIA, IIB, IV, V [29]. For compound **177**, it was obtained a precursor ion of *m/z* 295.1324 ($C_{19}H_{18}O_3$, error 3.6881 ppm) in $[M+H]^+$ mode at 67.86 min. As it shown in Fig. 4a, it yielded diagnostic ions at *m/z* 280.1087, 277.2156, 225.1270, 249.1270 which produced

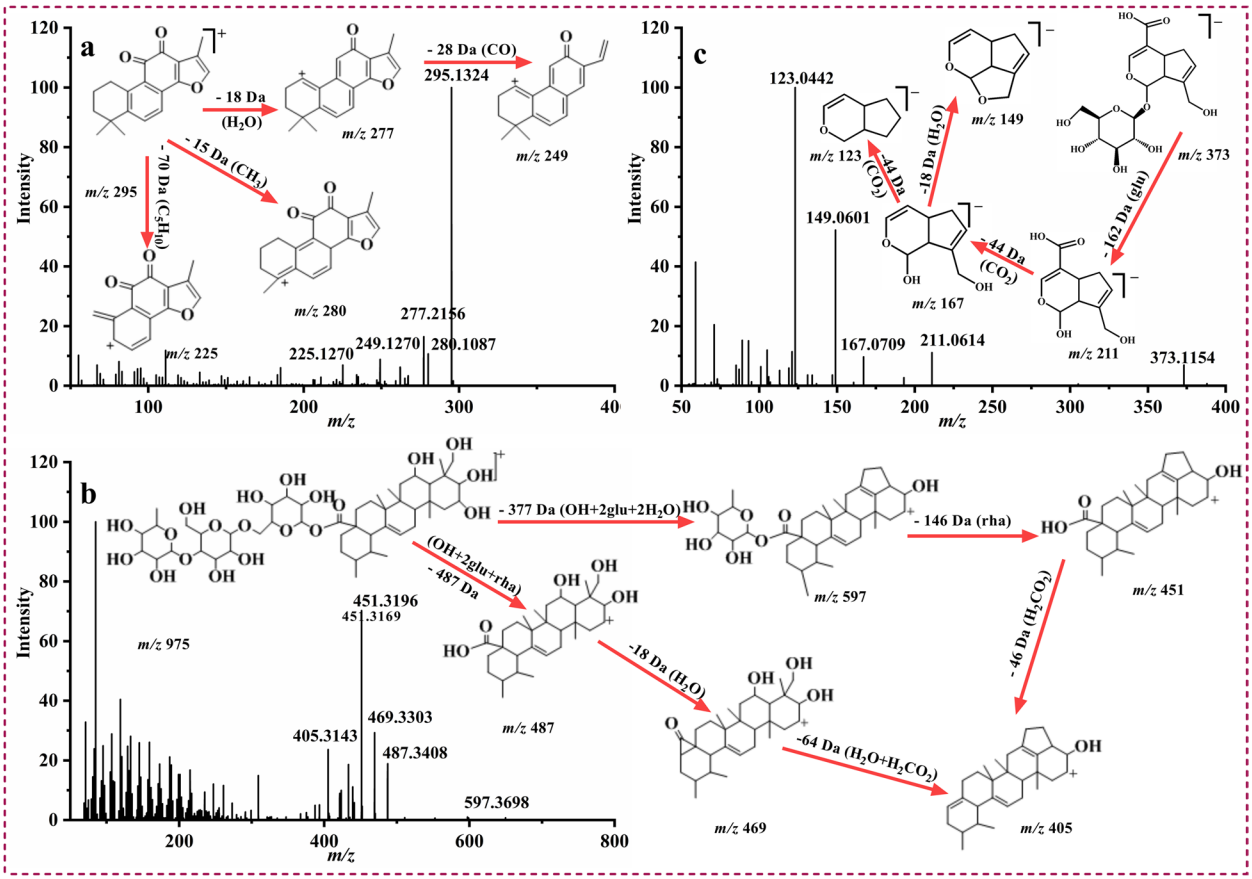

Fig. 4 The MS/MS spectra and fragmentation pathways of tanshinone IIA **a**, madecassoside **b** in positive ion mode, and geniposidic **c** in negative ion mode

by the loss of CH_3 (15 Da), H_2O (15 Da), C_5H_{10} (70 Da) and CO (28 Da). In comparison with the reference standard, compound **177** was precisely recognized as tanshinone IIA. In addition, triterpene compounds (compound **131**, **132**, **150**, **151**, **155**, **167**, **171**) in XL were presumably derived from Poria and CH, including poricoic acid class [30] and asiaticoside class [31]. Compound **132** generated a molecule ion *m/z* 975.5137 ($C_{48}H_{78}O_{20}$, error -1.2594 ppm) in $[M+H]^+$ mode with a high abundance. While the sugar group of triterpene glycosides were easily dropped, diagnostic ions *m/z* 597.3698 $[M+H\text{-}OH\text{-}glu\text{-}glu\text{-}H_2O\text{-}H_2O]^+$, 487.3408 $[M+H\text{-}glu\text{-}glu\text{-}rha\text{-}OH]^+$, 451.3169 $[M+H\text{-}OH\text{-}glu\text{-}glu\text{-}H_2O\text{-}H_2O\text{-}rha]^+$ were obtained from MS/MS spectra, which were formed by the continuous removal of glucose (162 Da) and rhamnose (146 Da). Fragments of *m/z* 469.3303 and 205.3143 formed by the continuous drop of H_2O (18 Da) and H_2CO_2 (46 Da) were observed (Fig. 4b). By contrast with the relevant literatures and the MS/MS data of reference standard, compound **132** was confirmed as madecassoside. For compound 14 as an example, the fragmentation pattern of iridoids (compound **14**, **20**, **25**, **28**, **80**) were described (Fig. 4c) [32]. In negative ion mode, compound **14** ($C_{16}H_{22}O_{10}$, error of 3.6587 ppm) produced a high abundance of precursor ion of *m/z* 373.1151 at retention time of 12.83 min. After removing a glucose, it displayed a fragment of *m/z* 211.0614 $[M\text{-}H\text{-}glu]^-$. Fragments of *m/z* 167.0709, 123.0442 and 149.0601 formed by the continuous removal of CO_2 (44 Da) and H_2O (18 Da) were observed. Compound **14** was conjectured as geniposidic acid based on its specific MS data with previous literatures. According to these fragmentation mechanism and rules, terpenoid components in XL were tentatively identified.

Characterization of organic acids

A total of 47 organic acids were preliminarily qualified from XL, including 16 salvianolic acids (compound **9**, **13**, **16**, **59**, **72**, **76**, **88**, **95**, **99**, **104**, **111**, **112**, **120**, **121**, **149** and **166**), 21 Chlorogenic acids (compounds **18**, **22**, **23**, **31**, **32**, **34**, **36**, **37**, **41**, **43**, **44**, **46**, **50**, **58**, **69**, **83**, **87**, **90**, **107**, **117**, **128**), and 10 other organic acids (compounds **1**, **2**, **5**, **10**, **17**, **19**, **21**, **24**, **40** and **108**).

Salvianolic acids are water-soluble components in SRR which mainly contains dimer, trimer, tetramer and its derivatives composed by danshensu and caffeic acid as structural units [33, 34]. Salvianolic acids can produced a molecular ion in negative mode $[M-H]^-$ with of high abundance, and there were some special fragments like $[M-H-C_9H_8O_4]^-$, $[M-H-C_9H_{10}O_5]^-$, $[M-H-H_2O]^-$, and $[M-H-CO_2]^-$ which were produced by the gradual drop of a danshensu ($C_9H_{10}O_5$, 198 Da), a caffeic acid ($C_9H_8O_4$, 180 Da), and H_2O (18 Da), CO (28 Da), CO_2 (44 Da) (Fig. 5a, b and c). Compound **120** as an example, the regular mass spectrometric pattern of salvianolic acids was explained. Compound **120** displayed an exact precursor ion of *m/z* 717.1474 ($C_{36}H_{30}O_{16}$, error 3.0757 ppm) with retention time of 60.16 min. The MS/MS spectra offered further information about its fragmentation pathways illustrated in Fig. 5a and d. In negative ion mode, compound **120** showed fragments of *m/z* 519.0944 $[M-H-C_9H_{10}O_5]^-$ and 321.0410 $[M-H-2C_9H_{10}O_5]^-$ generated by the continuous drop of a danshensu ($C_9H_{10}O_5$, 198 Da) in sequence. The fragments of *m/z* 339.0511 [M-H-caffeic acid]$^-$, 295.0618 [M-H-caffeic acid-CO_2]$^-$ and 185.0242 was formed by the elimination of a caffeic acid ($C_9H_8O_4$, 180 Da), a molecule CO_2 on *m/z* 339.0511, a catechol ($C_6H_6O_2$, 110 Da) from the remaining residue. Combining with its reference standard's MS/MS data and retention time, compound **120** was identified as salvianolic acid B.

Chlorogenic acid is a kind of phenolic acid, which is condensed from caffeic acid and quinic acid shown in Fig. 6a, therefore, the fragmentation pattern of chlorogenic acid have some common characteristics [35, 36]. Compound **41** revealed *m/z* 677.1739 $[M-H]^-$ at retention time of 27.94 min. There were a number of diagnostic product ions in MS/MS spectra shown in Fig. 6b, including *m/z* 515.1233, 353.0881, that produced by the successive loss of caffeic acid (162 Da). Fragments of *m/z* 191.0560 [quinic acid-H]$^-$ and 179.0345 [caffeic acid-H]$^-$, which were common for all chlorogenic acids, were observed. According to the precursor ion and characteristic fragments, compound **41** were supposed to be as tri-*O*- caffeoylquinic acid. Compound **32** displayed

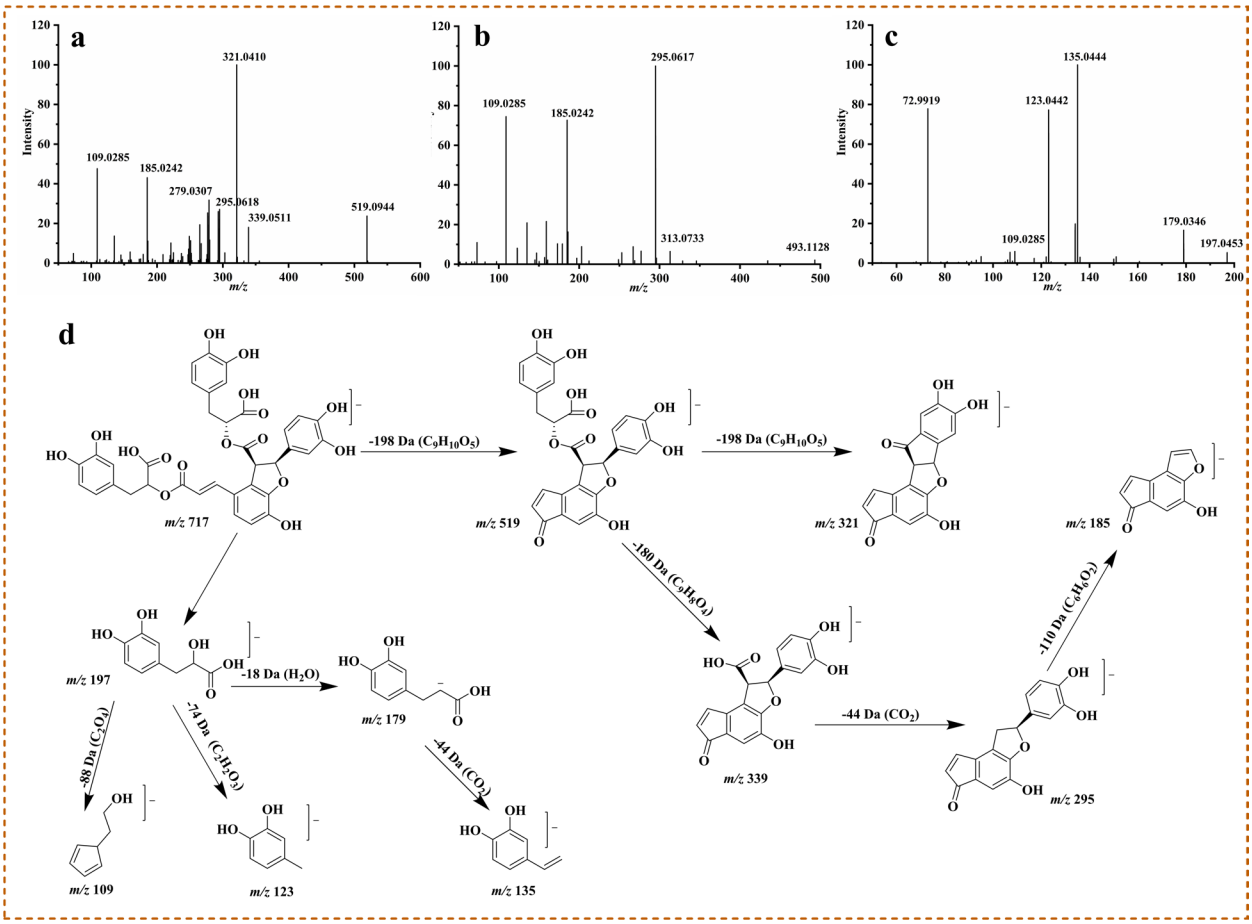

Fig. 5 The MS/MS spectra and main fragmentation pathways of salvianolic acid B **a**,**d**, salvianolic acid A **b**, danshensu **c** in negative ion mode

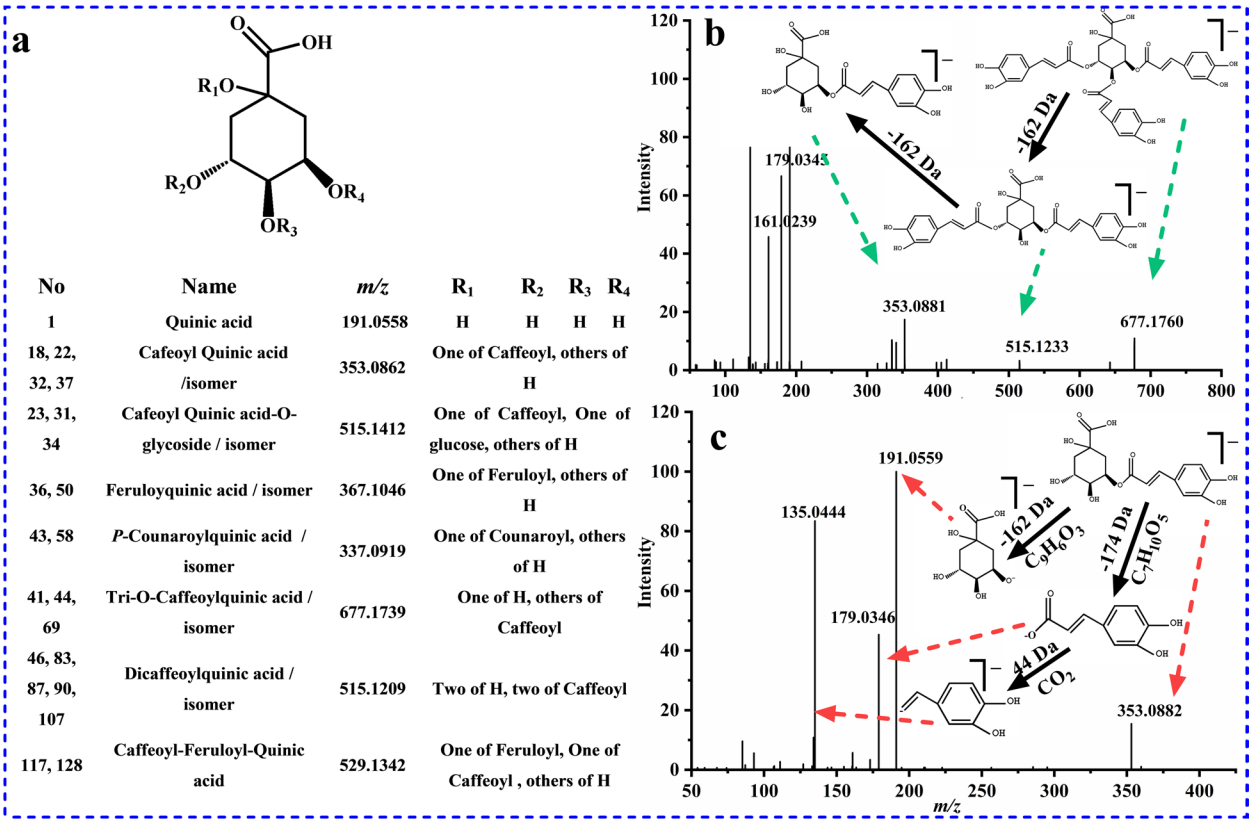

No	Name	*m/z*	R_1	R_2	R_3	R_4
1	Quinic acid	191.0558	H	H	H	H
18, 22, 32, 37	Cafeoyl Quinic acid /isomer	353.0862	One of Caffeoyl, others of H			
23, 31, 34	Cafeoyl Quinic acid-O-glycoside / isomer	515.1412	One of Caffeoyl, One of glucose, others of H			
36, 50	Feruloyquinic acid / isomer	367.1046	One of Feruloyl, others of H			
43, 58	*P*-Counaroylquinic acid / isomer	337.0919	One of Counaroyl, others of H			
41, 44, 69	Tri-O-Caffeoylquinic acid / isomer	677.1739	One of H, others of Caffeoyl			
46, 83, 87, 90, 107	Dicaffeoylquinic acid / isomer	515.1209	Two of H, two of Caffeoyl			
117, 128	Caffeoyl-Feruloyl-Quinic acid	529.1342	One of Feruloyl, One of Caffeoyl , others of H			

Fig. 6 The chemical structures of chlorogenic acids **a**, MS/MS spectra and main fragmentation pathways of tri-O- caffeoylquinic acid **b**, 4-O-caffeoyl quinic acid **c** in negative ion mode

precursor ions of *m/z* 353.0884 $[M-H]^-$ ($C_{16}H_{18}O_9$, error of 4.9037) and 707.1841 $[2\ M-H]^-$ with retention time of 24.53 min. Fragments of *m/z* 191.0559 [quinic acid-H]$^-$, 179.0346 [caffeic acid-H]$^-$, 135.0444 [caffeic acid-H-CO_2]$^-$ were obtained in MS/MS spectra (Fig. 6c). Compound **32** can be clearly marked as 4-*O*-caffeoyl quinic acid (cryptochlorogenic acid) by comparison with reference standard.

Characterization of flavonoids

Flavonoids are widely existing in various herbal plants, in this paper, a total of 25 flavonoids (compounds **62**, **66**, **70**, **71**, **74**, **75**, **84**, **92**, **93**, **97**, **105**, **130**, **133**, **138**, **158**, **159** in $[M-H]^-$ and compound **67**, **77**, **118**, **119**, **137**, **153**, **156**, **160**, **165** in $[M+H]^+$), mainly from SH [37], EC [38], AsR [39], were preliminarily identified according to their cleavage pattern combining with previous literatures on related components. Flavonoids in XL were including two types according to their flavone aglycones, flavonoids (Fig. 7a) and isoflavonoids (Fig. 7c). Either flavonoids or isoflavonoids or glycosyl flavonoids, they showed a similar fragmentation mechanism, such as removal of a glucose (162 Da), rhamnose (146 Da), glucuronic acid (176 Da) and losing some small neutral fragments H_2O (18 Da), CO_2 (44 Da), CO (28 Da), C_2H_2O (42 Da). Furthermore, RAD cleavage ions of *m/z* 151 or 137 were observed respectively from flavonoids and isoflavonoidsas well.

The major cleavage pattern of flavonoids was explained by the example of compound **70** and **67**, respectively. In $[M-H]^-$ mode, an accurate precursor ion of *m/z* 477.0684 ($C_{21}H_{17}O_{13}$, error 2.1756 ppm) were observed with a retention time of 37.02 min. The fragments of *m/z* 301.0358 [M-H-glcA]$^-$, 283.0269 [M-H-glcA-H_2O]$^-$, 255.0306 [M-H-glcA-H_2O]$^-$, 178.9981 [M-H-glcA-$C_7H_6O_2$]$^-$ were produced as characteristic fragments. And *m/z* 151.0030 was a special fragment ion from RAD cleavage. According to the relevant literatures and MS/MS data (Fig. 7b), compound **70** was presumed as quercetin-*O*-glucornide. Compound **67** exhibited a fragment of *m/z* 447.1282 ($C_{22}H_{22}O_{10}$, error 0.8251 ppm) in $[M+H]^+$ mode, at 35.99 min, showing an abundant feature fragment of *m/z* 285.0753 $[M+H\text{-glu}]^+$ in MS/MS spectra which was assignable to calycosin aglycone

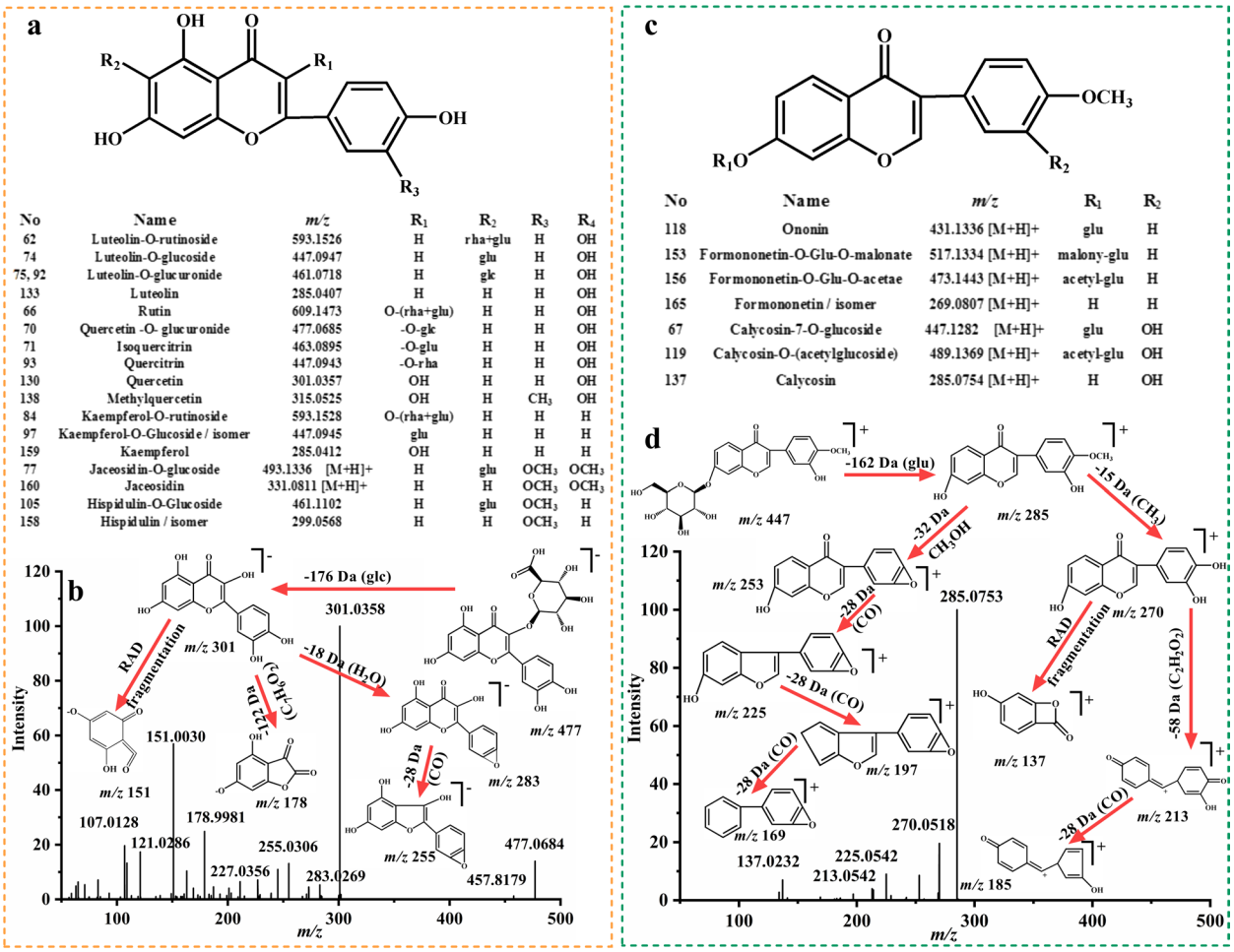

Fig. 7 The chemical structures flavonoids **a** and isoflavonoids **c**, the MS/MS spectra and fragmentation pathways of quercetin-O-glucornide **b** in negative ion mode, calycosin-7-O-glucoside **c** in positive ion mode

produced by the drop of a glucose (162 Da). At the same time, fragments were respectively obtained at *m/z* 270.0581 $[M+H\text{-glu-}CH_3]^+$, 253.0491 $[M+H\text{-glu-}CH_3OH]^+$, 213.0542 $[M+H\text{-glu-}CH_3\text{-}C_2H_2O_2]^+$ generated by the elimination of -CH_3 (15 Da), -OH (17 Da), $C_2H_2O_2$ (58 Da) moiety successively or simultaneously from precursor ion. Fragments of *m/z* 225.0542 $[M+H\text{-glu-}CH_3OH\text{-CO}]^+$, 197.0549 $[M+H\text{-glu-}CH_3OH\text{-2CO}]^+$, 169.0544 $[M+H\text{-glu-}CH_3OH\text{-3CO}]^+$ were generated by eliminating CO (28 Da) step by step. In addition, the most specific fragment formed by RDA cleavage observed at *m/z* 137.0232. Combining with the fragmentation pattern of reference standard, compound **67** was clearly marked as calycosin-7-*O*-glucoside (Fig. 7d).

Characterization of phenylethanoid glycosides (PhGs)

Phenylethanoid glycosides are the major active components in CDH [40, 41]. As it shown in Fig. 8a, the structure of PhGs are grouped by a phenylethyl alcohol, one or more glycoside and rhamnoside parts in conjunction with a phenolic acid such as caffeic acid, *p*-coumaric acid, ferulic acid. Therefore, PhGs demonstrate a similar fragments, after eliminating a phenolic acid (154 Da), glucose (162 Da) or rhamnose moiety (146 Da), and H_2O (18 Da), CO_2 (44 Da). Based on these characteristic fragment ions and previous reports on relevant components, a total of 29 PhGs (compound **29**, **38**, **42**, **54**, **57**, **61**, **64**, **68**, **80**, **81**, **86**, **94**, **98**, **100**, **102**, **104**, **109**, **110**, **113**, **114**, **115**, **116**, **123**, **125**, **126**, **136**, **140**, **144**, **152**) were preliminarily identified in XL.

For compound **57**, it demonstrated a precursor ion of *m/z* 785.2525 ($C_{35}H_{46}O_{20}$, error 3.1192 ppm) at

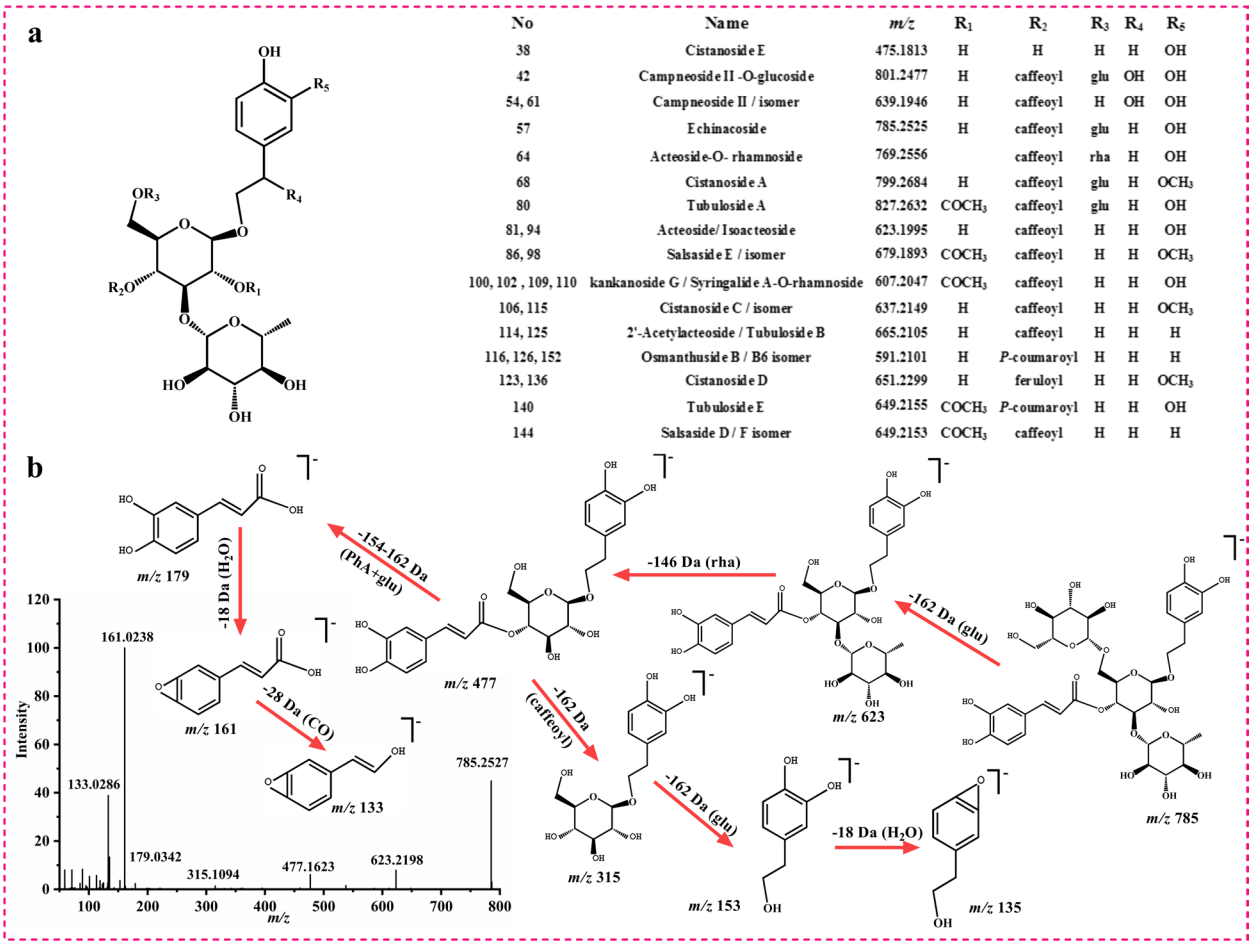

No	Name	*m/z*	R_1	R_2	R_3	R_4	R_5
38	Cistanoside E	475.1813	H	H	H	H	OH
42	Campneoside II -O-glucoside	801.2477	H	caffeoyl	glu	OH	OH
54, 61	Campneoside II / isomer	639.1946	H	caffeoyl	H	OH	OH
57	Echinacoside	785.2525	H	caffeoyl	glu	H	OH
64	Acteoside-O- rhamnoside	769.2556		caffeoyl	rha	H	OH
68	Cistanoside A	799.2684	H	caffeoyl	glu	H	OCH_3
80	Tubuloside A	827.2632	$COCH_3$	caffeoyl	glu	H	OH
81, 94	Acteoside/ Isoacteoside	623.1995	H	caffeoyl	H	H	OH
86, 98	Salsaside E / isomer	679.1893	$COCH_3$	caffeoyl	H	H	OCH_3
100, 102 , 109, 110	kankanoside G / Syringalide A-O-rhamnoside	607.2047	$COCH_3$	caffeoyl	H	H	OH
106, 115	Cistanoside C / isomer	637.2149	H	caffeoyl	H	H	OCH_3
114, 125	2'-Acetylacteoside / Tubuloside B	665.2105	H	caffeoyl	H	H	H
116, 126, 152	Osmanthuside B / B6 isomer	591.2101	H	*P*-coumaroyl	H	H	H
123, 136	Cistanoside D	651.2299	H	feruloyl	H	H	OCH_3
140	Tubuloside E	649.2155	$COCH_3$	*P*-coumaroyl	H	H	OH
144	Salsaside D / F isomer	649.2153	$COCH_3$	caffeoyl	H	H	H

Fig. 8 The chemical structures of PhGs **a**, the MS/MS spectra and main fragmentation pathways of echinacoside **b** in negative ion mode

$[M-H]^-$ mode. In the MS/MS spectra, the fragments of *m/z* 623.2198 $[M-H-glu]^-$, 477.1623 [M-H-caffeic acid-rha]$^-$, 315.1094 $[M-H-rha-caffeic\ acid]^-$ were observed, which were caused by continuous or synchronous elimination of a glucose (162 Da), a rhamnose (146 Da), and a caffeic acid (162 Da). It also showed fragments at *m/z* 161.0238 and 133.0186 produced from the gradual drop of phenylethyl alcohol ($C_8H_{10}O_3$, 154 Da) and CO (28 Da). Combining with the exact molecular mass and MS/MS fragments of reference standard, compound **57** were clearly recognized as echinacoside (Fig. 8b).

Characterization of the other types

Furthermore, a total of 31 other types of compounds, including 9 tannins (**4**, **7**, **8**, **11**,**12**, **15**, **35**, **45**, **60**), 4 lignans (**52**, **73**, **85**, **96**), 1 phenylpropanoids (**65**), 3 phenolic ketones (**56**, **63**, **162**), 2 sterones (**82**, **103**), 2 Benzylalcohol glycosides (**143**, **148**), 4 saponins (**161**, **163**, **164**, **170**), 2 lactones (**145**, **147**), 1 alkaloid (**129**) and others (**85**, **101**, **135**), were preliminarily characterized in XL combining with their accurate molecular weight, MS/MS spectra data and previous literature reports [42–45].

Discussion

In this work, a novel activity-directed chemical analysis strategy was established based on AR enzyme inhibition activity test for the fast and efficient analysis of chemical compounds in XL using UHPLC-Q-orbitrap-HRMS method. Firstly, in AR enzymatic reaction mode, the supernatant of XL showed higher inhibition activity than water extract and precipitates, which suggested that the chemical components with AR inhibition activity were mainly enriched in supernatant part of XL. In this experiment, a total of 178 compounds were identified and characterized from XL supernatant part, many of which were reported as the natural aldose redutase inhibitors with the better inhibition activity, such as quercetin [21], cryptotanshinone, tanshinoneIIA, tanshinone I [20],

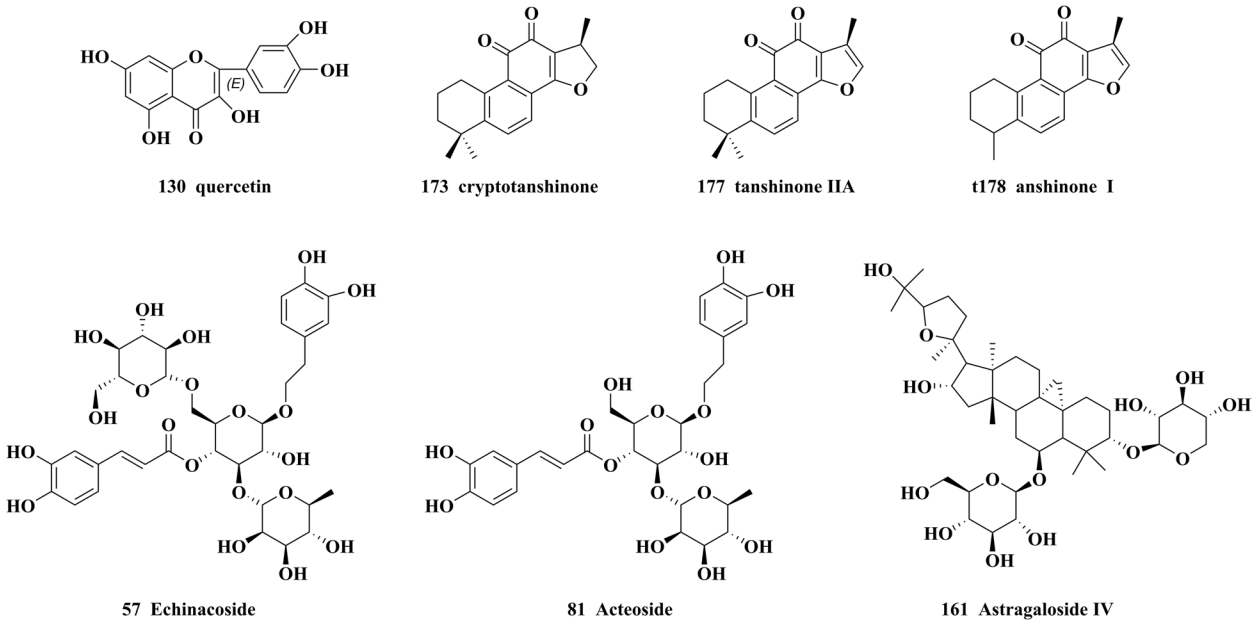

Fig. 9 The chemical structures of potential AR inhibitors in XL granule. Additionally, this study mainly summarized the fragmentation pathways of terpenes, organic acids, flavonoids, phenylethanoid glycosides in mass spectra.

echinacoside, acteoside [17], astragaloside IV [19] (chemical structures shown in Fig. 9). Therefore, we came to realize that they would be potentially active compounds in XL supernatant against AR.

Besides, comprehensive pharmacological studies found that, except AR inhibition activity, the most of 178 identified compounds in XL have better kidney protective effects [46, 47] with antioxidant [48], immune-modulating [49], and anti-inflammatory activities [50], especially, flavonoids and terpenes. The monoterpenoids in XL granules such as paeoniflorin (**55**), oxypaeoniflorin (**30**), were mainly from Paeoniae Radix Alba and Paeoniae Radix Rubra. There are some reports related with its pharmaceutical effects against DN. According to relevant reports, paeoniflorin (25–100 mg/kg) showed a significant renoprotective effect by inhibiting JAK2/STAT3 signaling pathway in diabetic mice [51]. Studies have suggested that paeoniflorin affects macrophage infiltration and activation in DN through TLR4 pathway, thereby improve clinical symptoms, delay the occurrence and development of DN [52]. It has been reported that paeoniflorin and oxypaeoniflorin have displayed therapeutic effects on DN by inhibiting oxidative damage and inflammation induced by advanced glycation end product in mesangial cells [53]. Furthermore, organic acids, such as chlorogenic acid and salvianolic acid, have been reported with renal protective effect on DN by in vivo and in vitro studies. It has been reported that chlorogenic acid can prevent diabetic nephropathy by inhibiting oxidative stress and inflammation through modulation of the Nrf2/HO-1 and NF-κB pathways [54]. Salvianolic acid B (**120**) can improve renal fibrosis and inflammation in diabetic nephropathy db/db mice through the regulation of TGF-beta1/Smad and NF-κB signaling pathways [55]. Furthermore, tanshinone IIA (**177**) showed a protective effect on the early stage of experimental DN [56]. The flavonoids in XL granule, including quercetin (**130**), kaempferol (**159**), quercetin-*O*-glucornide (**70**), calycosin-7-*O*-glucoside (**67**), rutin (**66**) and formononetin (**165**), have showed the renoprotection effect at different models [21, 57]. Echinacoside and acteoside in XL granule are the main active component of Cistanches Herba. More and more studies have confirmed that echinoside and acteoside have renal protective effects on DN [17]. In conclusion, the chemical components identified by LC–MS are the characteristic ingredients of each medicinal herb in XL, as well as the major compounds of XL granule with therapeutic effects on DN. Therefore, the chemical component analysis by LC–MS has preliminarily revealed the pharmacodynamic material basis of XL granule from the chemical point of view.

The preliminary study on XL extract precipitate part showed that the precipitate displayed a better immunoregulation effect [58]. These relevant researches explained that a variety of chemical components in XL work together by multiple pathways to protect the renal

function, and can be useful for the further study on the pharmacological mechanism of XL as well.

Conclusions

In summary, this study is the section of a series of material basis studies on the treatment of DN using XL granule. This work discovered potential AR active components in XL supernatant by UHPLC-Q-orbitrap-HRMS method coupling with in vitro experiments. On the basis of these studies, we will carry out further research on the mechanism of drug action. Our findings provide sufficient evidence to support the clinical application of XL granule, and more importantly, Theses experimental results can offer an analytical approach for the identification and characterization of complex TCM prescriptions, as well as explain a substantial basis for the pharmacological effect and quality control of XL.

Abbreviations

UHPLC-Q-orbitrap-HRMS	Ultra-high performance liquid chromatography coupled with quadrupole-orbitrap high resolution mass spectrometry
DN	Diabetic nephropathy
TCM	Traditional Chinese medicine
AR	Aldose reductase
TIC	Total ion chromatography
PhGs	Phenylethanoid glycosides
SH	Saussureae Involucratae Herba
CRH	Cibotii Rhizima
CR	Cyathulae Radix
EC	Eucommiae Cortex
AsR	Astragali Radix
SRR	Salviae Miltiorrhizae Radix et Rhizoma
MC	Moutan Cortex
PRR	Paeoniae Radix Rubra
PRA	Paeoniae Radix Alba
CDH	Cistanches Herba
CH	Centellae Herba

Supplementary Information

The online version contains supplementary material available at https://doi.org/10.1186/s12906-023-04025-5.

Additional file 1:Table S1. The informations of reference substances

Acknowledgements

This work was financially supported by the National Key R&D Program of China (No2020YFE0205600), and by "CAM Resources DataBase" in National Basic Science Data Center (NO. NBSDC-DB-19), also supported by Youth Innovation Promotion Association CAS and K.C. Wong Education Foundation.

Authors' contributions

Xiatiguli Taximaimaiti: Investigation, writing original draft preparation. Rahima Abdulla: nalidation, writing- reviewing and editing. Tao Wu, Yuan Zhao: project administration. Xuelei Xin, Yi Liu: methodology, writing- reviewing and editing. Haji Akber Aisa, Deqiang Deng: resources, supervision. All authors contributed and approved the manuscript.

Funding

Not applicable.

Availability of data and materials

All obtained data have been included in the manuscript.

Declarations

Ethics approval and consent to participate

Not applicable.

Consent for publication

Not applicable.

Competing interests

The authors declare that they have no competing interests.

Received: 27 January 2023 Accepted: 4 June 2023
Published online: 05 July 2023

References

1. Natesan V, Kim SJ. Diabetic nephropathy - a review of risk factors, progression, mechanism, and dietary management. Biomol Ther (Seoul). 2021;29:365–72.
2. Du Y, Xu BJ, Deng X, Wu XW, Li YJ, Wang SR, Wang YN, Jia S, Guo MZ, Yang DZ, Tang DQ. Predictive metabolic signatures for the occurrence and development of diabetic nephropathy and the intervention of *Ginkgo biloba* leaves extract based on gas or liquid chromatography with mass spectrometry. J Pharm Biomed Anal. 2019;166:30–9.
3. Zhao T, Zhang H, Zhao T, Zhang X, Lu J, Yin T, Liang Q, Wang Y, Luo G, Lan H, Li P. Intrarenal metabolomics reveals the association of local organic toxins with the progression of diabetic kidney disease. J Pharm Biomed Anal. 2012;60:32–43.
4. Shen YL, Wang SJ, Rahman K, Zhang LJ, Zhang H. Chinese herbal formulas and renal fibrosis: an overview. Curr Pharm Des. 2018;24:2774–81.
5. Wang Q, Tian X, Zhou W, Wang Y, Zhao H, Li J, Zhou X, Zhang H, Zhao T, Li P. Protective role of tangshen formula on the progression of renal damage in db/db mice by TRPC6/Talin1 pathway in podocytes. J Diabetes Res. 2020;2020:3634974.
6. Tokalı FS, Demir Y, Demircioğlu IH, Türkeş C, Kalay E, Şendil K, Beydemir Ş. Synthesis, biological evaluation, and in silico study of novel library sulfonates containing quinazolin-4(3H)-one derivatives as potential aldose reductase inhibitors. Drug Develop Res. 2023;83:586–604.
7. Sever B, Altıntop MD, Demir Y, Türkeş C, Özbaş K, Çiftçi GA, Beydemir Ş, Özdemir A. A new series of 2,4-thiazolidinediones endowed with potent aldose reductase inhibitory activity. Open Chem. 2021;19:347–57.
8. Belhassana A, Chtita S, Zaki H, Alaqarbehd M, Alsakhene N, Almohtaseb F, Lakhlifi T, Bouachrine M. In silico detection of potential inhibitors from vitamins and their derivatives compounds against SARS-CoV-2 main protease by using molecular docking, molecular dynamic simulation and ADMET profiling. J Mol Struct. 2022;1258: 132675.
9. Zhang H, Chen RY, Xu C, Zhang GM, Guan YX, Feng Q, Yao JC, Yan JZ. An integrated approach to discriminate the quality markers of Traditional Chinese medicine preparation based on multi-dimensional characteristic network: Shenqi Jiangtang Granule as a case. J Ethnopharmacol. 2021;278: 114277.
10. Shehzad MT, Hameed A, Al-Rashida M, Imran A, Uroos M, Asnuzilawati A, Mohamad H, Islam M, Iftikhar S, Shafiq Z, Iqbal J. Exploring antidiabetic potential of adamantyl-thiosemicarbazones via aldose reductase (ALR2) inhibition. Bioorg Chem. 2019;92: 103244.
11. Sarikaya M, Yazihan N, Evcimen ND. Relationship between aldose reductase enzyme and the signaling pathway of protein kinase C in an in vitro diabetic retinopathy model. Can J Physiol Pharmacol. 2020;98:243–51.
12. Türkeş C, Demir Y, Biçer A, Cin GT, Gültekin MS, Beydemir Ş. Exploration of some bis-sulfide and bis-sulfone derivatives as non-classical aldose reductase inhibitors. ChemistrySelect. 2023;8: e202204350.
13. Ertano BY, Demir Y, Nural Y, Erdoğan O. Investigation of the effect of acylthiourea derivatives on diabetes-associated enzymes. ChemistrySelect. 2022;7: e202204149.

14. Türkeş C, Arslan M, Demir Y, Çoçaj L, Nixha AR, Beydemir Ş. N-substituted phthalazine sulfonamide derivatives as non-classical aldose reductase inhibitors. J Mol Recognit. 2022;35: e2991.
15. Özaslan MS, Sağlamtaş R, Demir Y, Genç Y, Saraçoğlu İ, Gülçin İ. Isolation of some phenolic compounds from Plantago subulata L. and determination of their antidiabetic, anticholinesterase, antiepileptic and antioxidant Activity. Chem Biodivers. 2023;19:e202200280.
16. Türkeş C, Demir Y, Beydemir Ş. In vitro inhibitory activity and molecular docking study of selected natural phenolic compounds as AR and SDH inhibitors. ChemistrySelect. 2022;7: e202204050.
17. Morikawa T, Ninomiya K, Imamura M, Akaki J, Fujikura S, Pan Y, Yuan D, Yoshikawa M, Jia X, Li Z, Muraoka O. Acylated phenylethanoid glycosides, echinacoside and acteoside from *Cistanche tubulosa*, improve glucose tolerance in mice. J Nat Med. 2014;68:561–6.
18. Ha DT, Ngoc TM, Lee IS, Lee YM, Kim JS, Jung HJ, Lee SM, Na MK, Bae KH. Inhibitors of aldose reductase and formation of advanced glycation end-products in Moutan Cortex (*Paeonia suffruticosa*). J Nat Prod. 2009;72:1465–70.
19. Yin X, Zhang Y, Wu H. Zhu Xiang, Zheng X, Jiang S, Zhuo H, Shen J, Li L, Qiu J, Protective effects of Astragalus saponin I on early stage of diabetic nephropathy in rats. J Pharmacol Sci. 2004;95:256–66.
20. Kasimu R, Basnet P, Tezuka Y, Kadota S, Namba T. Danshenols A and B, New aldose reductase inhibitors from the root of *Salvia miltiorrhiza Bunge*. Chem Pharm Bull. 1997;45:564–6.
21. Oliveira TT, Nagem TJ, Miranda LCG, Paula VF, Teixeira MA. Inhibitory action on aldose reductase by Soybean flavonoids. J Braz Chem Soc. 1997;8:211–3.
22. Sun Z, Zhao M, Zuo L, Zhou S, Fan F, Jia Q, Xue L, Li H, Kang J, Zhang X. Rapid qualitative profiling and quantitative analysis of Juglandis Mandshuricae Cortex and seven flavonoids by ultra-high performance liquid chromatography-quadrupole/orbitrap high-resolution mass spectrometry. J Sep Sci. 2022;45:518–28.
23. Cao S, Hu M, Yang L, Li M, Shi Z, Cheng W, Zhang Y, Chen F, Wang S, Zhang Q. Chemical constituent analysis of *Ranunculus sceleratus* L. using ultra-high-performance liquid chromatography coupled with quadrupole-orbitrap high-resolution mass spectrometry. Molecules. 2022;27:3299.
24. Bai X, Liu Z, Tang T, Yu S, Liu D, Liu G, Fan X, Tang Y, Liu Z. An integrative approach to uncover the components, mechanisms, and functions of traditional Chinese medicine prescriptions on male infertility. Front Pharmacol. 2022;13: 794448.
25. Ye M, Li J, Tong F, Xin XL, Aisa HA. Optimization of microwave-assissted extraction using response surface methodology and the potential anti-diabetic efficacy of Nigella glandulifera Freyn determined using the spectrum-effect relationship. Ind Crop Prod. 2020;153: 112592.
26. Zhan ZL, Deng AP, Kang LP, Tang JF, Nan TG, Chen T, He YL, Guo LP, Huang LQ. Chemical profiling in Moutan Cortex after sulfuring and desulfuring processes reveals further insights into the quality control of TCMs by non-targeted metabolomic analysis. J Pharm Biomed Anal. 2018;156:340–8.
27. Huang Q, Chena JJ, Pan Y, He XF, Wang Y, Zhang XM, Geng CA. Chemical profiling and antidiabetic potency of Paeonia delavayi: comparison between different parts and constituents. J Pharm Biomed Anal. 2021;198: 113998.
28. Shi YH, Zhu S, Ge YW, Toume K, Wang ZT, Batkhuu J, Komatsu K. Characterization and quantification of monoterpenoids in different types of peony root and the related Paeonia species by liquid chromatography coupled with ion trap and time-of-flight mass spectrometry. J Pharm Biomed Anal. 2016;129:581–92.
29. Ma Z, Zhang M, Song Z. Characterization of tanshinones with quinone reductase induction activity from Radix Salvia miltiorrhiza by liquid chromatography/tandem mass spectrometry. Rapid Commun Mass Spectrom. 2009;23:2857–66.
30. Yang HM, Yang B, Hu YM, Cao L, Wang ZZ, Zhu KJ, Xiao W. Identification of chemical constituents in Guizhi Fuling Capsules by UPLC-Q-TOF-MS/MS. China J Chin Materia Med. 2020;45:861–77.
31. Masi F, Chianese G, Peterlongo F, Riva A, Taglialatela-Scafati O. Phytochemical profile of Centevita (R), a *Centella asiatica* leaves extract, and isolation of a new oleanane-type saponin. Fitoterapia. 2022;158: 105163.
32. Song Q, Zhou Z, Li J, Cao Y, Zhao Y, Deng S, Qi H, Jiang Y, Song Y, Tu P. Serial hyphenation of dried spot, reversed phase liquid chromatography, hydrophilic interaction liquid chromatography, and tandem mass spectrometry towards direct chemical profiling of herbal medicine-derived liquid matrices, an application in *Cistanche sinensis*. J Pharm Biomed Anal. 2019;174:34–42.
33. Zhu Z, Zhang H, Zhao L, Dong X, Li X, Chai Y, Zhang G. Rapid separation and identification of phenolic and diterpenoid constituents from Radix Salvia miltiorrhizae by high-performance liquid chromatography diode-array detection, electrospray ionization time-of-flight mass spectrometry and electrospray ionization quadrupole ion trap mass spectrometry. Rapid Commun Mass Spectrom. 2007;21:1855–65.
34. Xu T, Zuo L, Sun Z, Wang P, Zhou L, Lv X, Jia Q, Liu X, Jiang X, Zheng Z, Kang J, Zhang X. Chemical profiling and quantification of Shen-Kang injection, a systematic quality control strategy using ultra high performance liquid chromatography with Q exactive hybrid quadrupole orbitrap high-resolution accurate mass spectrometry. J Sep Sci. 2017;40:4872–9.
35. Zhang JY, Zhang Q, Li N, Wang ZJ, Lu JQ, Qiao YJ. Diagnostic fragment-ion-based and extension strategy coupled to DFIs intensity analysis for identification of chlorogenic acids isomers in Flos Lonicerae Japonicae by HPLC-ESI-MSn. Tlanta. 2013;104:1–9.
36. Gao D, Wang BJ, Huo ZP, He Y, Polachi N, Lei ZD, Liu XX, Song ZH, Qi LW. Analysis of chemical constituents in an herbal formula Jitong Ning Tablet. J Pharm Biomed Anal. 2017;140:301–12.
37. Jia Z, Wu C, Jin H, Zhang J. Identification of the chemical components of Saussurea involucrate by high-resolution mass spectrometry and the mass spectral trees similarity filter technique. Rapid Commun Mass Spectrom. 2014;28:2237–51.
38. Yan Y, Zhao H, Chen C, Zou L, Liu X, Chai C, Wang C, Shi J, Chen S. Comparison of multiple bioactive constituents in different parts of *Eucommia ulmoides* based on UFLC-QTRAP-MS/MS combined with PCA. Molecules. 2018;23:643.
39. Wang Y, Liu L, Ma Y, Guo L, Sun Y, Liu Q, Liu J. Chemical discrimination of *Astragalus mongholicus* and *Astragalus membranaceus* based on metabolomics using UHPLC-ESI-Q-TOF-MS/MS approach. Molecules. 2019;24:4064.
40. Chen XL, Deng ZT, Huang XY, Geng CA, Chen JJ. Liquid chromatography-mass spectrometry combined with xanthine oxidase inhibition profiling for identifying the bioactive constituents from *Cistanche deserticola*. Int J Mass Spectrom. 2018;430:1–7.
41. Li WL, Ding JX, Bai J, Hu Y, Song H, Sun XM, Ji YB. Research on correlation of compositions with oestrogenic activity of Cistanche based on LC/QTOF-MS/MS technology. Open Chem. 2019;17:1–12.
42. Wu YT, Huang WY, Lin TC, Sheu SJ. Determination of moutan tannins by high-performance liquid chromatography and capillary electrophoresis. J Sep Sci. 2003;26:1629–34.
43. Ren MT, Li HJ, Sheng LS, Liu P, Li P. Rapid analysis of constituents of Radix Cyathulae using hydrophilic interaction-reverse phase LC-MS. J Sep Sci. 2009;32:3988–95.
44. Qi X, Dong Y, Shan C, Xiang Y, Wang X. Analysis of the main components in herbal pair: Astragali Radix and Salviae Miltiorrhizae by UFLC-Q-TOF/MS. J Nanjing Univ Traditional Chinese Med. 2017;33:93–103.
45. Xiao W, Li X, Li N, Bolati M, Wang X, Jia X, Zhao Y. Sesquiterpene lactones from *Saussurea involucrate*. Fitoterapia. 2011;82:983–7.
46. Ding S, Wang W, Song X, Ma H. Based on network pharmacology and molecular docking to explore the underlying mechanism of Huangqi Gegen Decoction for treating diabetic nephropathy. Evid Based Complement Alternat Med. 2021;2021:9928282.
47. Shao YX, Gong Q, Qi XM, Wang K, Wu YG. Paeoniflorin ameliorates macrophage infiltration and activation by inhibiting the TLR4 signaling pathway in diabetic nephropathy. Front Pharmacol. 2019;10:566.
48. Benzarti S, Hamdi H, Lahmayer I, Toumi W, Kerkeni A, Belkadhi K, Sebei H. Total phenolic compounds and antioxidant potential of quince (*Cydonia oblonga Miller*) leaf methanol extract. Int J Innov Appl Stud. 2015;13:518–26.
49. Marefati N, Ghorani V, Shakeri F, Boskabady M, Kianian F, Rezaee R, Boskabady MH. A review of anti-inflammatory, antioxidant, and immunomodulatory effects of *Allium cepa* and its main constituents. Pharm Biol. 2021;59:287–302.
50. Tian XY, Li MX, Lin T, Qiu Y, Zhu YT, Li XL, Tao WD, Wang P, Ren XX, Chen LP. A review on the structure and pharmacological activity of phenylethanoid glycosides. Eur J Med Chem. 2021;209: 112563.

51. Li XY, Wang Y, Wang K, Wu YG. Renal protective effect of Paeoniflorin by inhibition of JAK2/STAT3 signaling pathway in diabetic mice. Biosci Trends. 2018;12:168–76.
52. Shao YX, Gong Q, Qi XM, Wang K, Wu YG. Paeoniflorin ameliorates macrophage infiltration and activation by inhibiting the TLR4 signaling pathway in Diabetic Nephropathy. Front Pharmacol. 2019;10:00566.
53. Zhang MH, Feng L, Zhu MM, Gu JF, Wu C, Jia XB. Antioxidative and anti-inflammatory activities of paeoniflorin and oxypaeoniflora on AGEs-Induced mesangial cell damage. Planta Med. 2013;79:1319–23.
54. Bao LP, Li JS, Zha DQ, Zhang L, Gao P, Yao T, Wu XY. Chlorogenic acid prevents diabetic nephropathy by inhibiting oxidative stress and inflammation through modulation of the Nrf2/HO-1 and NF-κB pathways. Int Immunopharmacol. 2018;54:245–53.
55. Gao HY, Bo Z, Wang Q, Luo L, Zhu HY, Ren Y. Salvanic acid B inhibits myocardial fibrosis through regulating TGF-β1/Smad signaling pathway. Biomed Pharmacother. 2019;110:685–91.
56. Kim SK, Jung KH, Lee BC. Protective effect of Tanshinone IIA on the early stage of experimental diabetic nephropathy. Biol Pharm Bull. 2009;32:220–4.
57. Tang T, He B, Zheng ZG, Wang RS, Gu F, Duan TT, Cheng HQ, Zhu Q. Inhibitory effects of two major isoflavonoids in Radix Astragali on high glucose-induced mesangial cells proliferation and AGEs-Induced endothelial cells apoptosis. Planta Med. 2011;77:729–32.
58. Li K, Li SY, Wang D, Li XX, Wu X, Liu XJ, Du GH, Li XR, Qin XM, Du YG. Extraction, characterization, antitumor and immunological activities of hemicellulose polysaccharide from Astragalus radix herb residue. Molecules. 2019;24:3644.

Publisher's Note